

Origin for the enhanced copper spin echo decay rate in the pseudogap regime of the multilayer high- T_c cuprates

Atsushi Goto^{1,2}, W. G. Clark¹, Patrik Vonlanthen¹, Kenji B. Tanaka¹, Tadashi Shimizu², Kenjiro Hashi², P. V. P. S. S. Sastry^{3,4}, and Justin Schwartz^{3,4}

¹*Department of Physics and Astronomy, University of California, Los Angeles, CA, 90095-1547*

²*National Institute for Materials Science, 3-13, Sakura, Tsukuba, Ibaraki, 305-0003, Japan*

³*National High Magnetic Field Laboratory, 1800 E. Paul Dirac Drive, Tallahassee, Florida 32310 and*

⁴*Department of Mechanical Engineering, FAMU-FSU College of Engineering, Tallahassee, Florida 32306*

(Dated: October 29, 2018)

We report measurements of the anisotropy of the spin echo decay for the inner layer Cu site of the triple layer cuprate, $\text{Hg}_{0.8}\text{Re}_{0.2}\text{Ba}_2\text{Ca}_2\text{Cu}_3\text{O}_8$ ($T_c=126$ K) in the pseudogap T regime below $T_{\text{pg}} \sim 170$ K and the corresponding analysis for their interpretation. As the field alignment is varied, the shape of the decay curve changes from Gaussian ($H_0 \parallel c$) to single exponential ($H_0 \perp c$). The latter characterizes the decay caused by the fluctuations of adjacent Cu nuclear spins caused by their interactions with electron spins. The angular dependence of the second moment ($T_{2M}^{-2} \equiv \langle \Delta\omega^2 \rangle$) deduced from the decay curves indicates that T_{2M}^{-2} for $H_0 \parallel c$, which is identical to T_{2G}^{-2} (T_{2G} is the Gaussian component), is substantially enhanced, as seen in the pseudogap regime of the bilayer systems. Comparison of T_{2M}^{-2} between $H_0 \parallel c$ and $H_0 \perp c$ indicates that this enhancement is caused by electron spin correlations between the inner and the outer CuO_2 layers. These results provide the answer to the long-standing controversy regarding the opposite T dependences of $(T_1T)^{-1}$ and T_{2G}^{-2} in the pseudogap regime of bi- and trilayer systems.

PACS numbers: 74.72.Gr, 74.25.Ha, 76.60.-k

The pseudogap phenomenon has been one of the central issues in understanding the anomalous normal states of high- T_c cuprates. Since the discovery of the pseudogap [1], NMR has continued to be a basic tool for its investigation. Temperature and doping dependences of the spin-lattice relaxation times (T_1) and the Knight shifts (K_s) of the Cu sites have served as crucial tests for the theories describing the pseudogap. A controversy, however, has arisen on the interpretation of the Gaussian component of a spin-spin relaxation time (T_{2G}). In systems such as $\text{YBa}_2\text{Cu}_3\text{O}_{6.6}$ and $\text{YBa}_2\text{Cu}_4\text{O}_8$, T_{2G}^{-2} continues to grow as T is lowered towards T_c , whereas $(T_1T)^{-1}$ decreases in the pseudogap regime [2, 3]. If the same dynamical susceptibility $\chi(\mathbf{q}, \omega)$ is responsible for both relaxation rates, an anomalous enhancement is expected at the high frequency part of $\text{Im}\chi(\mathbf{q}, \omega)$ in the pseudogap regime. This rather peculiar conclusion has puzzled theorists, and other explanations have been sought.

A key to resolve the problem is that the phenomenon is observed only in multilayer systems. One proposed mechanism is spin correlations between adjacent layers [4, 5, 6], which had been observed in spin echo double resonance (SEDOR) experiments [7, 8, 9]. They are expected to play essential roles in the systematic increase of T_c with increasing the number of layers because they can provide attractive forces between layers and stabilize the superconductivity [10]. In the bilayer systems, the two CuO_2 layers in a unit cell are equivalent, so that the Cu nuclei on one of the layers behave as like-spins to the others in the echo decay process, and contribute to T_{2G}^{-2} through the interlayer spin correlations. Unfortunately, since the contribution from the interlayer coupling is indistinguishable from its intralayer counterpart for the

identical layers, it is difficult to extract the effect experimentally in such systems.

In order to identify experimentally the interlayer effects on T_{2G} , we have utilized the trilayer cuprate $\text{Hg}_{0.8}\text{Re}_{0.2}\text{Ba}_2\text{Ca}_2\text{Cu}_3\text{O}_8$ ($T_c = 126$ K) with a pseudogap ($T_{\text{pg}} \sim 170$ K), where one inner and two outer CuO_2 layers are crystallographically inequivalent. This enables us to separate the interlayer effects from the total decay rates. In this letter, we report the measurements of the angular dependence of the second moment in the inner Cu site, which identifies the role of interlayer correlations in the echo decay process in the pseudogap regime of a multilayer system. Our analysis of the results shows that the different behavior of $(T_1T)^{-1}$ and T_{2G}^{-2} is caused by interlayer spin correlations.

The powder sample was prepared using the method of Ref. 11 and magnetically oriented along the c -axis. Figure 1 shows the angular dependence of the frequency spectrum for the ^{63}Cu central transition at 135 K. The angle θ is that between H_0 and the c -axis. Each curve was obtained by adding the real part of the FT spectra of the half echo measured at a few different frequencies [12]. The relatively narrow and wide lines are assigned to Cu(1) and Cu(2) sites in the inner and outer layers, respectively [13]. We confirmed that K_s and the quadrupole frequency (ν_Q) are consistent with previous results [14, 15]. The triangles in Fig. 1 indicate the positions at which echo decays were measured. Since the Cu(1) and Cu(2) lines overlap at 10° and 70° , both lines contribute to the measured decay.

The angular dependence of the echo decay curves at 135 K is shown in Fig. 2(a), where the Redfield contribution from T_1 has been removed by dividing the measured

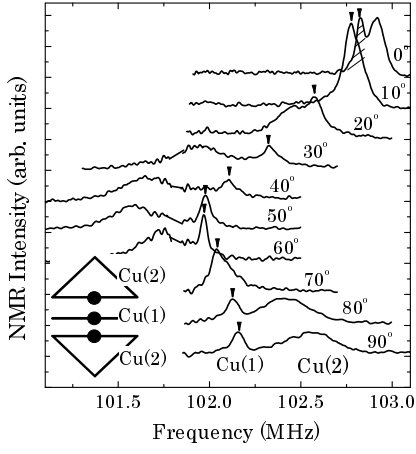


FIG. 1: Absorption spectra for the central transition of ^{63}Cu at 135 K as a function of θ . The triangles show the part of the spectra used for the T_2 measurements. Inset: Schematic view of the CuO layers

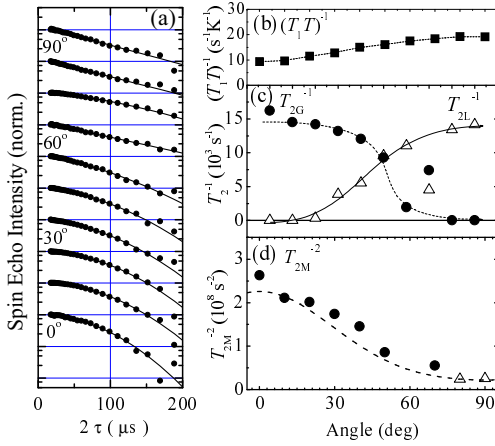


FIG. 2: Angular dependences of (a) the echo decay curve, (b) $(T_1T)^{-1}$, (c) T_{2G}^{-1} (\bullet) and T_{2L}^{-1} (Δ) in Eq. (3) and (d) T_{2M}^{-2} deduced from T_{2G}^{-2} (\bullet) and T_{2L}^{-2} (Δ) at 135 K. The dashed curve in (d) is given by Eq. (8).

data by $\exp(-2\tau/T_{1R})$ [16] with T_{1R} obtained as follows [17]. The general form of T_{1R}^{-1} is given by

$$(T_{1R})_z^{-1} = \{I(I+1) - 1/4\}(W_x + W_y) + W_z, \quad (1)$$

where W_γ ($\gamma=x, y, z$) is from the spin fluctuations in the γ direction and z is the quantization axis ($\parallel H_0$). In the same notation, $(T_1)_z^{-1}$ is given by $(T_1)_z^{-1} = W_x + W_y$. Hence, for an arbitrary θ ,

$$[T_{1R}(\theta)]^{-1} = \{I(I+1) - 1/4\}[T_1(\theta)]^{-1} + [T_1(90^\circ - \theta)]^{-1} - 0.5[T_1(0^\circ)]^{-1}, \quad (2)$$

where the relation $W_a = W_b$ is used (The subscripts a, b correspond to the crystalline axes). From the anisotropy of $(T_1T)^{-1}$ in Fig. 2(b), $[T_{1R}(\theta)]^{-1}$ is calculated.

Figure 2(a) shows that the shape of the decay curve changes from Gaussian at 0° to single exponential

(Lorentzian spectrum) at 90° . These data are fitted by the function,

$$\frac{M(2\tau)}{e^{-2\tau/T_{1R}}} = M_0 \exp \left[-\frac{2\tau}{T_{2L}} - \frac{1}{2} \left(\frac{2\tau}{T_{2G}} \right)^2 \right] \quad (3)$$

with M_0 , T_{2L} and T_{2G} as free parameters. The angular dependences of T_{2L}^{-1} and T_{2G}^{-1} thus obtained are shown in Fig. 2(c). For $0^\circ \sim 20^\circ$, T_{2L}^{-1} is nearly zero while T_{2G}^{-1} is zero at 80° and 90° . In between, the decay curve crosses over between these two extremes. This change is a result of the NMR line narrowing caused by the following mechanism. At finite T the effective interaction between adjacent nuclear spins is reduced because of rapid spin flips driven by the hyperfine interaction with the electrons, which averages out the nuclear fields at adjacent nuclear sites. As a result, the central part of the NMR line is narrowed and the spectrum approaches a Lorentzian rather than a Gaussian shape [17, 18]. The importance of the effect depends on the ratio between the two time scales T_1 and $T_{2M} \equiv \langle \Delta\omega^2 \rangle^{-1/2}$, where $\langle \Delta\omega^2 \rangle$ is the homogeneous second moment of the NMR absorption. The former and the latter characterize the time scales of the nuclear spin fluctuations and the echo decays, respectively.

There are two limiting cases where analytical forms for the decays are known. One is the static limit ($T_1/T_{2M} \gg 1$), where nuclear spins do not change their states between pulses or a pulse and an echo because of the relatively long T_1 . Consequently, the contributions from unlike-spins are canceled out at the time of the echo and only like-spins contribute to the echo decay. The decay in this case is described by a Gaussian [2],

$$\frac{M(2\tau)}{e^{-2\tau/T_{1R}}} = M_0 \exp \left[-\frac{1}{2} \left(\frac{2\tau}{T_{2M}} \right)^2 \right] f(2\tau), \quad (4)$$

where $f(2\tau)$ is the correction for the narrowing effect [19] and in the static limit, $f(2\tau) \equiv 1$. The rate T_{2M}^{-1} in this case is usually referred to as the Gaussian rate, T_{2G}^{-1} .

The second is the narrowed limit ($T_1/T_{2M} \leq 1$), where nuclei are fluctuating during the echo sequence. The decay is characterized by a single exponential (Lorentzian spectrum) [17, 18],

$$\frac{M(2\tau)}{e^{-2\tau/T_{1R}}} = M_0 \exp \left[-2\tau \left(\frac{63T_1}{63T_{2M}^2} + \frac{65T_1}{65T_{2M}^2} \right) \right], \quad (5)$$

where $\alpha T_{2M}^{-2} \equiv \alpha \langle \Delta\omega^2 \rangle$ is the contribution from the α -nuclei ($\alpha=63, 65$) to the second moment of ^{63}Cu , and αT_1 is the spin-lattice relaxation time in the α -site. Note that $^{63}T_{2M}$ corresponds to T_{2G} in the static limit. Here, ^{65}Cu also contributes to the ^{63}Cu decay because they lose their memories of the initial states during the echo sequence due to the fluctuation effect, so that their contributions are not canceled out at the time of the ^{63}Cu echo.

In the present case, the transition from the static to the narrowing regime is caused by the large anisotropies of T_1^{-1} and T_{2M}^{-1} . As will be shown later, T_{2M}^{-1} decreases

by 3.3 from $\theta = 0^\circ$ to 90° , while T_1^{-1} increases by 2.1. Also, there is a qualitative correspondence between the transition of the decay curve in Fig. 2(a) and the simulations by Walstedt et al. for the various values of T_1/T_{2M} (Fig. 4 of Ref 17). The angular dependence of T_{2M}^{-2} deduced from either T_{2G} or T_{2L} in Fig. 2(c) is shown in Fig. 2(d), where $T_{2M} = T_{2G}$ while Eq. (5) is used to obtain ${}^{63}T_{2M}$ from T_{2L} along with the relations,

$$\begin{aligned} ({}^{63}\gamma)^2 \cdot {}^{63}T_1 &= ({}^{65}\gamma)^2 \cdot {}^{65}T_1, & (6) \\ {}^{65}c \cdot ({}^{65}\gamma_n \cdot {}^{65}T_{2M})^2 &= {}^{63}c \cdot ({}^{63}\gamma_n \cdot {}^{63}T_{2M})^2, & (7) \end{aligned}$$

where ${}^\alpha c$ is the natural abundance for the isotope α .

The angular dependence of T_{2M}^{-2} in Fig. 2(d) is consistent with that of the hyperfine coupling constant. In the detuned limit, the flip-flop term ($I_i^+ I_j^-$) in the nuclear Hamiltonian is ineffective because of the mismatch in the Zeeman energies between adjacent nuclei. Hence, T_{2M}^{-2} is given only by the z-component term ($I_i^z I_j^z$), so that $[T_{2M}(\theta)]^{-2} \propto \{\chi(\mathbf{Q})\}^2 \cdot \sum_q \{F_q(\theta)\}^2$, where $F_q(\theta)$ is the form factor when H_0 is in the θ direction [3]. Here, we assume that the q-dependence of $\chi(\mathbf{q})$ around $\mathbf{Q} \equiv (\pi, \pi)$ is weaker than that of F_q , so that $\chi(\mathbf{q})$ is represented by $\chi(\mathbf{Q})$ and taken out of the q-summation. We further assume that $\sum_q \{F_q(\theta)\}^2$ is proportional to $\{F_q(\theta)\}^2$ at each θ . Since the θ dependence of $F_q(\theta)$ is $\{A(3 \cos^2 \theta - 1) + B\}^2$ where A and B are constants, the anisotropy of T_{2M}^{-2} is given by

$$[T_{2M}(\theta)]^{-2}/[T_{2M}(90^\circ)]^{-2} = (\sin^2 \theta + \xi \cos^2 \theta)^4, \quad (8)$$

where

$$\xi \equiv \left[\frac{\sum_q \{F_q(0^\circ)\}^2}{\sum_q \{F_q(90^\circ)\}^2} \right]^{1/4} \approx \left[\frac{F_{\mathbf{Q}}(0^\circ)}{F_{\mathbf{Q}}(90^\circ)} \right]^{1/2}. \quad (9)$$

The value of ξ can be estimated from the anisotropy of T_1^{-1} . Since $\chi(\mathbf{Q}) \gg \chi(0)$ in this system, $(T_1)_z^{-1} \propto \{F_x(\mathbf{Q}) + F_y(\mathbf{Q})\}$ [14]. Hence, ξ is given by,

$$\xi \approx \left[\frac{F_{\mathbf{Q}}(0^\circ)}{F_{\mathbf{Q}}(90^\circ)} \right]^{1/2} \approx \left[2 \frac{(T_1(90^\circ))^{-1}}{(T_1(0^\circ))^{-1}} - 1 \right]^{1/2}. \quad (10)$$

From Fig. 2(b), $(T_1(90^\circ))^{-1}/(T_1(0^\circ))^{-1} = 2.1$, so that $\xi=1.79$. The dashed curve in Fig. 2(d) shows the anisotropy of T_{2M}^{-2} obtained from Eq. (8) with $[T_{2M}(90^\circ)]^{-2}$ as a single adjustable parameter. It has the same tendency as the angular dependence of T_{2G}^{-2} in spite of some assumptions.

The analysis at 0° , 10° and 70° is not straightforward because of the overlap with the Cu(2) line. Since T_{2M}^{-1} at Cu(2) is expected to be smaller than that of Cu(1) by a factor of 0.75 [14], the overlapped Cu(2) line reduces T_{2M}^{-1} . T_{2M}^{-2} , however, is not reduced at 10° , and is significantly enhanced at 0° . At 70° , the shape of the decay curve itself is quite different from those at 60° and 80° . Below, we show that these features can be attributed to the interlayer spin correlations, which have the effect of enhancing T_{2M}^{-1} [4, 6].

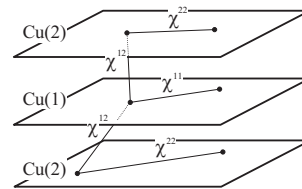


FIG. 3: Schematic view of the intra ($i = j$) and interlayer ($i \neq j$) spin susceptibilities ($\chi^{ij}(\mathbf{q})$) in the trilayer system.

Consider the echo decay process at $\theta = 0^\circ$. As seen in Fig. 1, the Cu(1) and Cu(2) lines are situated close to each other, so that not only Cu(1) but also a part of Cu(2) nuclei are excited, which also act as like-spins for the Cu(1) nuclei in the echo decay process. On the other hand, the intensity of the echo is obtained by integrating only the Cu(1) part of the FT spectrum of the echo (shaded part of the spectrum in Fig. 1), so that only the Cu(1) nuclei contribute to the intensity of the decay curve in Fig. 2(a). This is the same situation as that in the SEDOR experiment where the π -pulses for like- and unlike-spins are applied simultaneously. Since all the like-spins contribute to the Gaussian decay in the static limit, $[T_{2M}(0^\circ)]^{-2}$ is given by [6],

$$[T_{2M}(0^\circ)]^{-2} \propto \sum_q [F_q(0^\circ) \{\chi^{11}(\mathbf{q}) + 4\epsilon \chi^{12}(\mathbf{q})\}]^2, \quad (11)$$

where, χ^{11} and χ^{12} are the intra- and interlayer spin susceptibilities associated with the auto- and cross-correlations within or between layers indicated in Fig. 3. The second term in Eq. (11) corresponds to the contribution due to the interlayer correlations. The ratio of the excited Cu(2) nuclei (ϵ) is estimated to be about 0.6.

At the angles where the two Cu lines are separated from each other, the second term in Eq. (11) does not appear in the echo decay process, whereas at 10° and 70° , both the Cu(1) and Cu(2) nuclei are excited and observed, so that the second term in Eq. (11) also appears, which enhances T_{2M}^{-2} . This enhancement increases T_1/T_{2M} , and brings the situation at 70° closer to the static limit, resulting in the appearance of the Gaussian component in the decay curve. At 10° , a cancellation may occur between the reduction due to the overlapped Cu(2) line and the enhancement due to the interlayer spin correlations.

Figure 4(b) shows the T dependences of T_{2M}^{-2} at 0° and 90° , which are quite different from each other; i.e., while $[T_{2M}(90^\circ)]^{-2}$ starts to decrease at T_{pg} as does $(T_1 T)^{-1}$ shown in Fig. 4(a), $[T_{2M}(0^\circ)]^{-2}$ continues to grow down to T_c . This difference is caused by the χ^{12} term in Eq. (11). Provided again that the q-dependences of $\chi^{ij}(\mathbf{q})$ around \mathbf{Q} are weaker than that of F_q , T_{2M}^{-2} at 0° and 90°

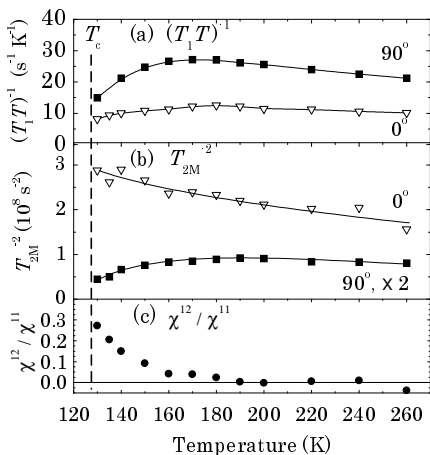


FIG. 4: T dependences of (a) $(T_1 T)^{-1}$ and (b) T_{2M}^{-2} at 0° and $2T_{2M}^{-2}$ at 90° . (c) $\chi^{12}(\mathbf{Q})/\chi^{11}(\mathbf{Q})$ defined by Eq. (14).

can be rewritten as [6, 13],

$$\begin{aligned}
 [T_{2M}(0^\circ)]^{-2} &\propto \{\chi^{11}(\mathbf{Q}) + 4\epsilon\chi^{12}(\mathbf{Q})\}^2 \cdot \sum_q \{F_q(0^\circ)\}^2, \\
 [T_{2M}(90^\circ)]^{-2} &\propto \{\chi^{11}(\mathbf{Q})\}^2 \cdot \sum_q \{F_q(90^\circ)\}^2.
 \end{aligned} \quad (12)$$

Here, we define the ratio ρ by,

$$\rho \equiv \frac{[T_{2M}(0^\circ)]^{-2}}{[T_{2M}(90^\circ)]^{-2}} \cdot \xi^{-4} = \left[1 + 4\epsilon \frac{\chi^{12}(\mathbf{Q})}{\chi^{11}(\mathbf{Q})} \right]^2, \quad (13)$$

which gives,

$$\chi^{12}(\mathbf{Q})/\chi^{11}(\mathbf{Q}) = (\sqrt{\rho} - 1)/4\epsilon. \quad (14)$$

The T dependence of $\chi^{12}(\mathbf{Q})/\chi^{11}(\mathbf{Q})$ calculated from ρ is shown in Fig. 4(c), where ξ is adjusted so that $\rho = 1$ at high T . One can see that $\chi^{12}(\mathbf{Q})/\chi^{11}(\mathbf{Q})$ rapidly increases in the pseudogap T region, indicating that $\chi^{12}(\mathbf{Q})$ rapidly grows there. This is consistent with the SEDOR results [7, 8, 9] and the theoretical calculations [5, 6, 20, 21, 22]. Note that $\chi^{12}(\mathbf{Q})/\chi^{11}(\mathbf{Q}) \approx T_{2S}^{-1}/T_{2G}^{-1}$ where T_{2S} is the SEDOR decay time between the sites on the different layers. From Fig. 4(d), we find that,

$$\chi^{12}(\mathbf{Q})/\chi^{11}(\mathbf{Q}) = 0.28, \quad (15)$$

at T_c , while T_{2S}^{-1}/T_{2G}^{-1} was reported to be about 0.25 at T_c in $\text{Y}_2\text{Ba}_4\text{Cu}_7\text{O}_{15}$. [8] The consistent explanation for both T_{2M}^{-1} and T_{2S}^{-1} indicates that they can be interpreted on the same basis of the interlayer spin correlations.

In conclusion, we have investigated the anisotropy of the spin echo decay in the inner Cu site of the trilayer cuprate $\text{Hg}_{0.8}\text{Re}_{0.2}\text{Ba}_2\text{Ca}_2\text{Cu}_3\text{O}_8$ to obtain the anisotropy of the second moment T_{2M}^{-2} . Comparison between the data at 0° and 90° shows the rapid growth of $\chi^{12}(\mathbf{Q})$ in the pseudogap regime. Since this is a common effect in multilayer systems, we conclude that the opposite T dependences between $(T_1 T)^{-1}$ and T_{2G}^{-2} observed in the pseudogap regime of bilayer systems are caused by interlayer spin correlations. The UCLA part of the work was supported by NSF Grant DMR-0072524.

-
- [1] H. Yasuoka, T. Shimizu, T. Imai, S. Sasaki, Y. Ueda, and K. Kosuge, *Hyp. Int.* **49**, 167 (1989).
 - [2] Y. Itoh et al., *J. Phys. Soc. Jpn.* **61**, 1287 (1992).
 - [3] M. Takigawa, *J. Phys. Chem. Solids* **53**, 1651 (1992).
 - [4] J. Kishine, Thesis, University of Tokyo (1996).
 - [5] J. Kishine, *Physica C* **282-287**, 1771 (1997).
 - [6] A. Goto and T. Shimizu, *Phys. Rev. B* **57**, 7977 (1998).
 - [7] R. Stern, M. Mali, J. Roos, and D. Brinkmann, *Phys. Rev. B* **52**, R15734 (1995).
 - [8] A. Suter, M. Mali, J. Roos, and D. Brinkmann, *Phys. Rev. Lett.* **82**, 1309 (1999).
 - [9] B. W. Statt, L. M. Song, and C. E. Bird, *Phys. Rev. B* **55**, 11122 (1997).
 - [10] M. U. Ubbens and P. A. Lee, *Phys. Rev. B* **50**, 438 (1994).
 - [11] P. V. P. S. S. Sastry et al., *Physica C* **297**, 223 (1998).
 - [12] W. G. Clark, M. E. Hanson, F. Lefloch, and P. Ségransan, *Rev. Sci. Instrum.* **66**, 2453 (1995).
 - [13] A. Goto, T. Shimizu, P. V. P. S. S. Sastry, and J. Schwartz, *Phys. Rev. B* **59**, R14169 (1999).
 - [14] K. Magishi et al., *J. Phys. Soc. Jpn.* **64**, 4561 (1995).
 - [15] M.-H. Julien et al., *Phys. Rev. Lett.* **76**, 4238 (1996).
 - [16] A. G. Redfield, *IBM J. Res. Dev.* **1**, 19 (1957).
 - [17] R. E. Walstedt and S.-W. Cheong, *Phys. Rev. B* **51**, 3163 (1995).
 - [18] A. Abragam, *The Principles of Nuclear Magnetism* (Oxford University Press, New York, 1961).
 - [19] N. J. Curro, T. Imai, C. P. Slichter, and B. Dabrowski, *Phys. Rev. B* **56**, 877 (1997).
 - [20] H. Monien and T. M. Rice, *Physica C* **235-240**, 1705 (1994).
 - [21] G. Hildebrand, E. Arrigoni, J. Schmalian, and W. Hanke, *Phys. Rev. B* **59**, R685 (1999).
 - [22] A. Goto and T. Shimizu, *Physica B* **259-261**, 468 (1999).